
<https://doi.org/10.15407/ujpe66.12.1027>

B. ALEMU,¹ CH. GASHU,² E. MOSISA,² T. ABEBE¹

¹ Department of Physics, Adama Science and Technology University
(P. O. Box 1888, Adama, Ethiopia; e-mail: tam1704@gmail.com)

² Department of Physics, Jimma University
(P. O. Box 378, Jimma, Ethiopia; e-mail: tam1704@gmail.com)

DYNAMICS OF THE CAVITY RADIATION OF A CORRELATED EMISSION LASER COUPLED TO A TWO-MODE THERMAL RESERVOIR

In this paper, the quantum properties of the cavity light beam produced by a coherently driven nondegenerate three-level laser with an open cavity and coupled to a two-mode thermal reservoir are thoroughly analyzed. We have carried out our analysis by putting the noise operators associated with the thermal reservoir in normal order. Here we discussed more the effect of thermal light and the spontaneous emission on the dynamics of the quantum processes. It is found that the maximum degree of intracavity squeezing 43% below the vacuum-state level. Moreover, the presence of thermal light leads to decrease the degree of entanglement.

Keywords: stimulated emission, photon statistics, quadrature squeezing, spontaneous emission.

1. Introduction

Three-level cascade lasers have received considerable attention over the years in connection with the strong correlation between the modes of the generated radiation that leads to a substantial degree of nonclassical features [1–27]. When a three-level atom in a cascade configuration makes a transition from the top to the bottom level via the intermediate level, two photons are generated. If the two photons have the same frequency, then the three-level atom is called a degenerate three-level atom. Otherwise, it is called nondegenerate. The squeezing and statistical properties of the light produced by three-level lasers, when the atoms are initially prepared in a coherent superposition of the top and bottom levels or when these levels are coupled by a strong coherent light, have been studied by several authors [28–39]. These authors have found that these quantum optical systems can generate squeezed light under certain conditions.

Moreover, Abebe [11] has studied the squeezing and entanglement properties of the light generated by a coherently driven nondegenerate three-level laser possessing an open cavity and coupled to a two-mode vacuum reservoir. He showed that the maximum quadrature squeezing of the light generated by the laser, operating below the threshold, is found to be 50% below the vacuum-state level. Moreover, Abebe [27] also studied the quantum properties of the light produced by a coherently driven nondegenerate three-level laser with a closed cavity and coupled to a two-mode vacuum reservoir. In this study, he found that the maximum quadrature squeezing is 43% below the vacuum-state level, which is slightly less than the result found on an open cavity [11]. He also found that the photon numbers of two-mode light beams are correlated. The analysis in [27] showed that the intracavity quadrature squeezing is enhanced due to the driven coherent light. It is found that the squeezing and entanglement in the two-mode light are directly related. As a result, an increase in the degree of squeezing directly implies

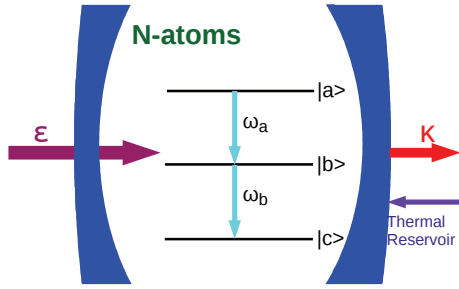


Fig. 1. (Color online) Schematic representation of a coherently driven nondegenerate three-level laser coupled to a two-mode thermal reservoir

an increase in the degree of entanglement. This shows that whenever there is the squeezing in the two-mode light, there exists the entanglement in the system.

In this paper, we will study the quantum properties of the cavity light beams produced by a coherently driven nondegenerate three-level laser with an open cavity and coupled to a two-mode thermal reservoir via a single-port mirror. First, we obtain the master equation for a coherently driven nondegenerate three-level atom with the cavity modes and the quantum Langevin equations for the cavity mode operators. Employing the master equation and the long-time approximation scheme, we drive the equations of evolution of the expectation values of the atomic operators. Hence, we determine the steady-state solutions of the resulting equations of evolution. Here, we carry out our calculation by putting the noise operators associated with the two-mode thermal reservoir in normal order. Applying the steady-state solutions of the resulting equations of evolution along with the quantum Langevin equations, we obtain the quadrature squeezing, the entanglement of photon and cavity atomic-states, the mean photon number, the photon number correlations, and the variance of a difference of intensities.

2. Operator Dynamics

We consider the case in which N nondegenerate three-level atoms in the cascade configuration are available in an open cavity. We denote the top, intermediate, and bottom levels of the three-level atom by $|a\rangle_k$, $|b\rangle_k$, and $|c\rangle_k$, respectively. As shown in Fig. 1 for the nondegenerate cascade configuration, when the atom makes a transition from level $|a\rangle_k$ to $|b\rangle_k$ and from levels $|b\rangle_k$ to $|c\rangle_k$, two photons with different frequencies are emitted. The emission of light, when the atoms

makes the transition from the top level to the intermediate level, is light mode a , and the emission of light, when the atom makes the transition from the intermediate level to the bottom level, is light mode b . We assume that the cavity mode a is at resonance with transition $|a\rangle_k \rightarrow |b\rangle_k$, and the cavity mode b is at resonance with the transition $|b\rangle_k \rightarrow |c\rangle_k$, with the top and bottom levels of a three-level atom coupled by coherent light. The interaction of a three-level atom with the cavity modes and the driving coherent light can be described by the Hamiltonian

$$\hat{H}_S = ig[\hat{\sigma}_a^{\dagger k} \hat{a} - \hat{a}^\dagger \hat{\sigma}_a^k + \hat{\sigma}_b^{\dagger k} \hat{b} - \hat{b}^\dagger \hat{\sigma}_b^k] + \frac{i\Omega}{2} [\hat{\sigma}_c^{\dagger k} - \hat{\sigma}_c^k], \quad (1)$$

where g is the coupling constant between the atom and cavity mode a or b , \hat{a} and \hat{b} are the annihilation operators for light modes a and b , and

$$\hat{\sigma}_a^k = |b\rangle_k \langle a|, \quad \hat{\sigma}_b^k = |c\rangle_k \langle b|, \quad \hat{\sigma}_c^k = |c\rangle_k \langle a| \quad (2)$$

are lowering atomic operators. Here, $\Omega = 2\varepsilon\lambda$, in which ε , considered to be real and constant, is the amplitude of the driving coherent light, and λ is the coupling constant between the driving coherent light and the three-level atom.

2.1. The master equation

In order to study the dynamics of the cavity radiation of the combined system, it is necessary to obtain the relevant equations of evolution. To begin, the contribution of the initial thermal light in the cavity and the two-mode vacuum reservoir to the master equation is sought. To this end, one can start with the well-established fact that the time evolution of the reduced density operator for the cavity radiation coupled to a reservoir has, in the Born approximation [28], the form

$$\begin{aligned} \frac{d}{dt} \hat{\rho}(t) = & -i[\hat{H}_S(t), \hat{\rho}(t)] - i[\langle \hat{H}_{SR}(t) \rangle_R, \hat{\rho}(0)] - \\ & - \int_0^t [\langle \hat{H}_{SR}(t) \rangle_R, [\hat{H}_S(t'), \hat{\rho}(t')]] dt' - \\ & - \int_0^t Tr_R [\hat{H}_{SR}(t), [\hat{H}_{SR}(t'), \hat{\rho}(t') \hat{R}]] dt', \end{aligned} \quad (3)$$

where S and R refer to the system and reservoir variables, and $\hat{\rho}(0)$ represents the radiation initially in the

cavity. The interaction Hamiltonian for N nondegenerate three-level atoms coupled to thermal reservoir is

$$\hat{H}_{SR}(t) = i \sum_j \lambda_j [\hat{\sigma}_a^{\dagger k} \hat{a}_j - \hat{a}_j^{\dagger} \hat{\sigma}_a^k + \hat{\sigma}_b^{\dagger k} \hat{b}_j - \hat{b}_j^{\dagger} \hat{\sigma}_b^k], \quad (4)$$

where λ_j is the coupling constant for the j^{th} mode of the reservoir, (\hat{a}_j, \hat{b}_j) are the annihilation operators of the two-mode thermal reservoir. Now, using the density operator of the thermal reservoir

$$\hat{R} = \sum_{n=0}^{\infty} \frac{\bar{n}_{\text{th}}^n}{(1 + \bar{n}_{\text{th}})^{n+1}} |n\rangle\langle n|, \quad (5)$$

one can easily check that

$$\begin{aligned} \langle \hat{a}_j \rangle_R &= \sum_{n=0}^{\infty} \frac{\bar{n}_{\text{th}}^n}{(1 + \bar{n}_{\text{th}})^{n+1}} \text{Tr}_R(|n\rangle\langle n| \hat{a}_j) = \\ &= \sum_{n=0}^{\infty} \frac{\bar{n}_{\text{th}}^n}{(1 + \bar{n}_{\text{th}})^{n+1}} \langle n|n-2\rangle = 0. \end{aligned} \quad (6)$$

Following the same procedure, we obtain

$$\begin{aligned} \langle \hat{b}_j \rangle_R &= \langle \hat{a}_j^2 \rangle = \langle \hat{b}_j^2 \rangle = \langle \hat{a}_j^{\dagger} \hat{b}_j \rangle_R = 0, \\ \langle \hat{b}_j^{\dagger} \hat{a}_j \rangle_R &= \langle \hat{a}_j \hat{b}_j \rangle_R = \langle \hat{b}_j \hat{a}_j \rangle_R = 0. \end{aligned} \quad (7)$$

In view of these results, we see that

$$\langle \hat{H}_{SR}(t) \rangle_R = 0. \quad (8)$$

Therefore, the second commutation relation in Eq. (3) is zero. This confirms that the thermal light in the cavity does not directly contribute to the master equation. In addition, applying the commutation relation $[\hat{a}_j, \hat{a}_j^{\dagger}] = 1$, we note that $\langle \hat{a}_j \hat{a}_j^{\dagger} \rangle = \bar{n}_{\text{th}} + 1$ and $\langle \hat{a}_j^{\dagger} \hat{a}_j \rangle = \bar{n}_{\text{th}}$, where $\bar{n}_a = \bar{n}_b = \bar{n}_{\text{th}}$ is the mean photon number for the thermal reservoir. As a result, solving the remaining terms by following the standard approach yields [2]

$$\begin{aligned} \frac{d}{dt} \hat{\rho}(t) &= g [\hat{\sigma}_a^{\dagger k} \hat{a} \hat{\rho} - \hat{a}^{\dagger} \hat{\sigma}_a^k \hat{\rho} + \hat{\sigma}_b^{\dagger k} \hat{b} \hat{\rho} - \hat{b}^{\dagger} \hat{\sigma}_b^k \hat{\rho} - \hat{\rho} \hat{\sigma}_a^{\dagger k} \hat{a} + \\ &+ \hat{\rho} \hat{a}^{\dagger} \hat{\sigma}_a^k - \hat{\rho} \hat{\sigma}_b^{\dagger k} \hat{b} + \hat{\rho} \hat{b}^{\dagger} \hat{\sigma}_b^k] + \frac{\Omega}{2} [\hat{\sigma}_c^{\dagger k} \hat{\rho} - \hat{\sigma}_c^k \hat{\rho} - \hat{\rho} \hat{\sigma}_c^{\dagger k} + \\ &+ \hat{\rho} \hat{\sigma}_c^k] + \frac{\gamma}{2} \bar{n}_{\text{th}} [2\hat{\sigma}_a^{\dagger k} \hat{\rho} \hat{\sigma}_a^k - \hat{\sigma}_a^k \hat{\sigma}_a^{\dagger k} \hat{\rho} - \hat{\rho} \hat{\sigma}_a^k \hat{\sigma}_a^{\dagger k}] + \\ &+ \frac{\gamma}{2} (\bar{n}_{\text{th}} + 1) [2\hat{\sigma}_a^k \hat{\rho} \hat{\sigma}_a^{\dagger k} - \hat{\sigma}_a^{\dagger k} \hat{\sigma}_a^k \hat{\rho} - \hat{\rho} \hat{\sigma}_a^{\dagger k} \hat{\sigma}_a^k] + \\ &+ \frac{\gamma}{2} \bar{n}_{\text{th}} [2\hat{\sigma}_b^{\dagger k} \hat{\rho} \hat{\sigma}_b^k - \hat{\sigma}_b^k \hat{\sigma}_b^{\dagger k} \hat{\rho} - \hat{\rho} \hat{\sigma}_b^k \hat{\sigma}_b^{\dagger k}] + \\ &+ \frac{\gamma}{2} (\bar{n}_{\text{th}} + 1) [2\hat{\sigma}_b^k \hat{\rho} \hat{\sigma}_b^{\dagger k} - \hat{\sigma}_b^{\dagger k} \hat{\sigma}_b^k \hat{\rho} - \hat{\rho} \hat{\sigma}_b^{\dagger k} \hat{\sigma}_b^k], \end{aligned} \quad (9)$$

where $\gamma_a = \gamma_b = \gamma = 2h\lambda^2$, considered to be the same for levels $|a\rangle$ and $|b\rangle$, is the spontaneous emission decay constant.

2.2. Quantum Langevin equations

We recall that the laser cavity is coupled to a two-mode thermal reservoir via a single-port mirror. In addition, we carry out our calculation by putting the noise operators associated with the thermal reservoir in normal order. Thus, the noise operators will not have any effect on the dynamics of the cavity mode operators [2, 11, 27]. Therefore, we can drop the noise operators and write the quantum Langevin equations for the operators \hat{a} and \hat{b} as

$$\frac{d\hat{a}}{dt} = -\frac{\kappa}{2} \hat{a} - i[\hat{a}, \hat{H}], \quad (10)$$

$$\frac{d\hat{b}}{dt} = -\frac{\kappa}{2} \hat{b} - i[\hat{b}, \hat{H}], \quad (11)$$

where κ is the cavity damping constant. Then in view of Eq. (1), the quantum Langevin equations for the cavity mode operators \hat{a} and \hat{b} turn out to be

$$\frac{d\hat{a}}{dt} = -\frac{\kappa}{2} \hat{a} - g\hat{\sigma}_a^k, \quad (12)$$

$$\frac{d\hat{b}}{dt} = -\frac{\kappa}{2} \hat{b} - g\hat{\sigma}_b^k. \quad (13)$$

Following the procedure described by Abebe [11, 27], for N atoms, we have

$$\frac{d\hat{a}}{dt} = -\frac{\kappa}{2} \hat{a} + \frac{g}{\sqrt{N}} \hat{m}_a, \quad (14)$$

$$\frac{d\hat{b}}{dt} = -\frac{\kappa}{2} \hat{b} + \frac{g}{\sqrt{N}} \hat{m}_b. \quad (15)$$

The sum of Eqs. (14) and (15) yields

$$\frac{d\hat{c}}{dt} = -\frac{\kappa}{2} \hat{c} + \frac{g}{\sqrt{N}} \hat{m}. \quad (16)$$

Employing the master equation (9) and following a straightforward algebra described by [11, 27], it is possible to obtain the steady-state solution of the stochastic differential equation of the atomic operators

$$\langle \hat{N}_a \rangle = \left[\frac{\Omega^2}{(\gamma_c + \gamma)^2 (\bar{n}_{\text{th}} + 1) (2\bar{n}_{\text{th}} + 1) + 3\Omega^2} \right] N, \quad (17)$$

$$\langle \hat{N}_b \rangle = \left[\frac{\Omega^2}{(\gamma_c + \gamma)^2 (\bar{n}_{\text{th}} + 1) (2\bar{n}_{\text{th}} + 1) + 3\Omega^2} \right] N, \quad (18)$$

$$\langle \hat{N}_c \rangle = \left[\frac{(\gamma_c + \gamma)^2 (\bar{n}_{\text{th}} + 1) (2\bar{n}_{\text{th}} + 1) + \Omega^2}{(\gamma_c + \gamma)^2 (\bar{n}_{\text{th}} + 1) (2\bar{n}_{\text{th}} + 1) + 3\Omega^2} \right] N, \quad (19)$$

$$\langle \hat{m}_c \rangle = \left[\frac{\Omega(\gamma_c + \gamma)(\bar{n}_{\text{th}} + 1)}{(\gamma_c + \gamma)^2 (\bar{n}_{\text{th}} + 1) (2\bar{n}_{\text{th}} + 1) + 3\Omega^2} \right] N. \quad (20)$$

3. Quadrature Squeezing

The squeezing properties of the two-mode cavity light are described by two quadrature operators

$$\hat{c}_+ = \hat{c}^\dagger + \hat{c}, \quad (21)$$

$$\hat{c}_- = i(\hat{c}^\dagger - \hat{c}), \quad (22)$$

where \hat{c}_+ and \hat{c}_- are Hermitian operators representing the physical quantities called plus and minus quadratures, respectively, while $\hat{c} = \hat{a} + \hat{b}$ is the annihilation operator for the two-mode cavity light. To this end, the two quadrature operators satisfy the commutation relation

$$[\hat{c}_-, \hat{c}_+] = 2i \frac{\gamma_c}{\kappa} [\hat{N}_a - \hat{N}_c]. \quad (23)$$

In view of this result, the uncertainty relation for the plus and minus quadrature operators of the two-mode cavity light is

$$\Delta c_+ \Delta c_- \geq \frac{\gamma_c}{\kappa} |\langle \hat{N}_a \rangle - \langle \hat{N}_c \rangle|. \quad (24)$$

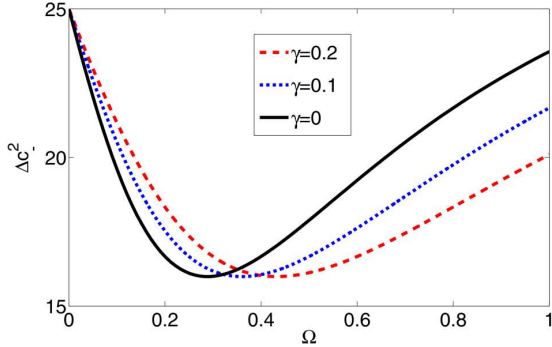


Fig. 2. (Color online). Plots of Δc_{\pm}^2 [Eq. (29)] versus Ω for $\gamma_c = 0.4$, $\kappa = 0.6$, $N = 50$, $\bar{n}_{th} = 0.2$ and for different values of γ

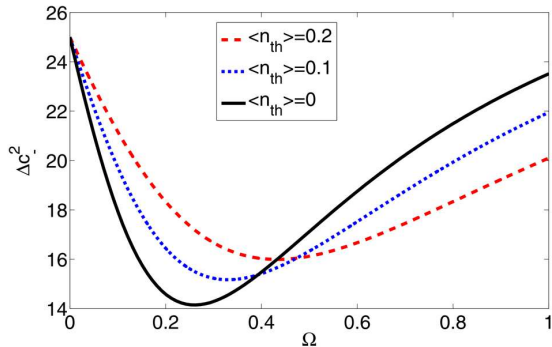


Fig. 3. (Color online). Plots of Δc_{\pm}^2 [Eq. (29)] versus Ω for $\gamma_c = 0.4$, $\kappa = 0.6$, $N = 50$, $\gamma = 0.2$ and for different values of \bar{n}_{th}

With regard for Eqs. (17) and (19), one can find

$$\Delta c_+ \Delta c_- \geq \frac{\gamma_c}{\kappa} N \left| \frac{(\gamma_c + \gamma)^2 (\bar{n}_{th} + 1) (2\bar{n}_{th} + 1)}{(\gamma_c + \gamma)^2 (\bar{n}_{th} + 1) (2\bar{n}_{th} + 1) + 3\Omega^2} \right|. \quad (25)$$

In the case where the coherent light is absent, ($\Omega = 0$), it is possible to see that

$$\Delta c_+ \Delta c_- \geq \frac{\gamma_c}{\kappa} N. \quad (26)$$

This is the minimum uncertainty relation for the two-mode cavity vacuum state.

In view of Eqs. (21) and (22), the variance of the plus and minus quadrature operators of the two-mode cavity light can be described as

$$\Delta c_{\pm}^2 = \langle \hat{c} \hat{c}^\dagger \rangle + \langle \hat{c}^\dagger \hat{c} \rangle \pm \langle \hat{c}^2 \rangle \pm \langle \hat{c}^{\dagger 2} \rangle \mp \langle \hat{c} \rangle^2 \mp \langle \hat{c}^\dagger \rangle^2 - 2 \langle \hat{c} \rangle \langle \hat{c}^\dagger \rangle. \quad (27)$$

Then it follows that

$$\Delta c_{\pm}^2 = \frac{\gamma_c}{\kappa} [N + \langle \hat{N}_b \rangle \pm 2 \langle \hat{m}_c \rangle]. \quad (28)$$

With regard for Eqs. (18) and (20), the quadrature variance of the two-mode cavity light in a steady state takes the form

$$\Delta c_{\pm}^2 = \left(\frac{\gamma_c}{\kappa} N \right) \left[\frac{(\gamma_c + \gamma)^2 (\bar{n}_{th} + 1) (2\bar{n}_{th} + 1)}{(\gamma_c + \gamma)^2 (\bar{n}_{th} + 1) (2\bar{n}_{th} + 1) + 3\Omega^2} + \frac{4\Omega^2 \pm 2\Omega(\gamma_c + \gamma)(\bar{n}_{th} + 1)}{(\gamma_c + \gamma)^2 (\bar{n}_{th} + 1) (2\bar{n}_{th} + 1) + 3\Omega^2} \right]. \quad (29)$$

In the case where $\Omega = 0$, it is not difficult to verify that

$$(\Delta c_+)_v^2 = (\Delta c_-)_v^2 = \frac{\gamma_c}{\kappa} N, \quad (30)$$

which is the normally ordered quadrature variance of the two-mode cavity light in the vacuum state. It is also observed that the uncertainties in the plus and minus quadratures are equal and satisfy the minimum uncertainty relation.

The plots in Fig. 2 present the quadrature variance of the two-mode cavity light beams versus Ω for $\gamma_c = 0.4$, $N = 50$, $\kappa = 0.8$, $\bar{n}_{th} = 0.2$ and for different values of γ . These plots show that the minimum value of the quadrature variance for $\gamma = 0.2$, $\gamma = 0.1$, and $\gamma = 0$ is $\Delta c_{\pm}^2 = 16$ and occurs at $\Omega = 0.4343$, $\Omega = 0.3636$, and $\Omega = 0.2929$, respectively. Moreover,

from the plots of the same figure, we observe that the quadrature variance increases with the spontaneous emission decay constant with the same value of Ω .

Furthermore, Fig. 3 shows the quadrature variance of the two-mode cavity light beams versus Ω for $\gamma_c = 0.4$, $\gamma = 0.2$ and for different values of \bar{n}_{th} . In Fig. 3, we see that the minimum values of the quadrature variance for $\bar{n}_{th} = 0.5$, $\bar{n}_{th} = 0.2$, and $\bar{n}_{th} = 0$ are $\Delta c_-^2 = 16$, $\Delta c_-^2 = 15.17$, and $\Delta c_-^2 = 14.14$ and occur at $\Omega = 0.4343$, $\Omega = 0.3232$, and $\Omega = 0.2626$, respectively.

The result presented in Fig. 4 indicates that the quadrature variance increases with a decrease in γ and Ω , since more atoms are expected to participate in the spontaneous emission process. It is also not difficult to realize from Fig. 5 that the degree of squeezing increases, when \bar{n}_{th} decreases. The maximum degree of squeezing occurs at the point, where the minimum quadrature variance occurs. Therefore, from this plot, the maximum degree of squeezing is found to be 62.4% when $\bar{n}_{th} = 0$ and occurs at $\Omega = 0.2929$. This result indicates that the presence of thermal light decreases the degree of quadrature squeezing.

Next, we proceed to calculate the quadrature squeezing of the two-mode cavity light in the entire frequency interval relative to the quadrature variance of the two-mode vacuum state. We define the quadrature squeezing of the two-mode cavity light by

$$S = \frac{(\Delta c_-)_v^2 - \Delta c_-^2}{(\Delta c_-)_v^2}. \quad (31)$$

In view of Eqs. (29) and (30), the quadrature squeezing of the two-mode cavity light turns out to have the form

$$S = \left[\frac{2\Omega(\gamma_c + \gamma)(\bar{n}_{th} + 1) - \Omega^2}{(\gamma_c + \gamma)^2(\bar{n}_{th} + 1)(2\bar{n}_{th} + 1) + 3\Omega^2} \right]. \quad (32)$$

We observe from this equation that, unlike the quadrature variance, the quadrature squeezing does not depend on the number of atoms. This implies that the quadrature squeezing of the two-mode cavity light is independent of the number of atoms.

In addition, we consider the case where the spontaneous emission and the thermal reservoir is absent ($\bar{n}_{th} = \gamma = 0$). Then the quadrature squeezing in this case takes the form

$$S = \left[\frac{2\Omega\gamma_c - \Omega^2}{\gamma_c^2 + 3\Omega^2} \right]. \quad (33)$$

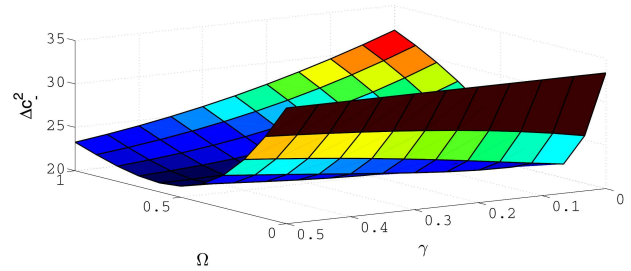


Fig. 4. (Color online). A plot of Δc_-^2 [Eq. (29)] versus Ω and γ for $\gamma_c = 0.4$, $\kappa = 0.6$, $N = 50$, and $\bar{n}_{th} = 0.2$

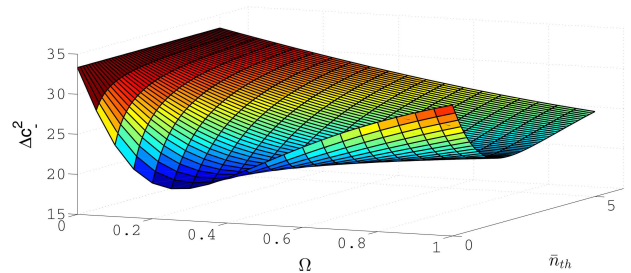


Fig. 5. (Color online). A plot of Δc_-^2 [Eq. (29)] versus Ω and \bar{n}_{th} for $\gamma_c = 0.4$, $\kappa = 0.6$, $N = 50$, and $\gamma = 0.2$

This result is exactly the same as the one obtained by Abebe [27].

The plots on Fig. 6 indicate the quadrature squeezing versus Ω for $\gamma_c = 0.4$, $\bar{n}_{th} = 0.2$, and for different values of γ . From these plots, we find that the maximum quadrature squeezing to be the same in the presence and in the absence of spontaneous emission. The plots in Fig. 6 show that the quadrature squeezing for $\gamma = 0$ is greater than for $\gamma = 0.1$ in the interval $0 \leq \Omega \leq 0.36$, and the quadrature squeezing for $\gamma = 0$ is less than for $\gamma = 0.1$ for $\Omega > 0.361$. The quadrature squeezing, when $\gamma = 0$, is greater than when $\gamma = 0.2$ in the interval $0 \leq \Omega \leq 0.38$, and the quadrature squeezing for $\gamma = 0$ is less than for $\gamma = 0.2$ for $\Omega > 0.38$. Moreover, the plots in the same figure show that the quadrature squeezing, when $\gamma = 0.1$, is greater than when $\gamma = 0.2$ in the interval $0 \leq \Omega \leq 0.4$, and the quadrature squeezing, when $\gamma = 0.1$, is less than when $\gamma = 0.2$ for $\Omega > 0.4$. Furthermore, from the same plots, the maximum squeezing is found to be 36% for $\gamma = 0.2$ (dashed curve), for $\gamma = 0.1$ (dotted curve), and for $\gamma = 0$ (solid curve) below the vacuum-state level. This occurs, when the three-level laser is operating at $\Omega = 0.4343$, $\Omega = 0.3636$, and $\Omega = 0.2929$, respectively.

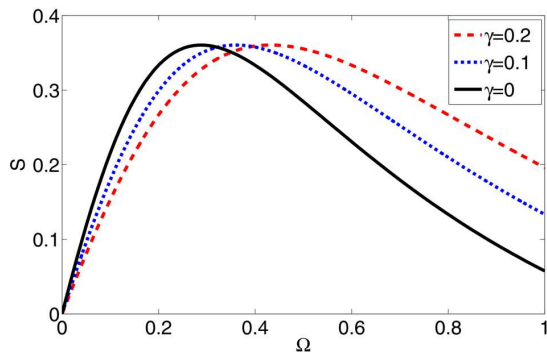


Fig. 6. (Color online). Plots of the quadrature squeezing [Eq. (32)] versus Ω for $\gamma_c = 0.4$, $\bar{n}_{th} = 0.2$, and for different values of γ

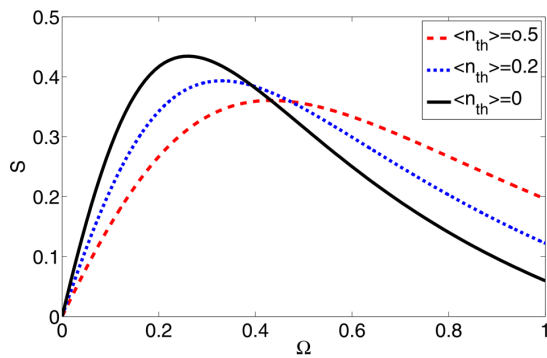


Fig. 7. (Color online). Plots of the quadrature squeezing [Eq. (32)] versus Ω for $\gamma_c = 0.4$, $\gamma = 0.2$, and for different values of \bar{n}_{th}

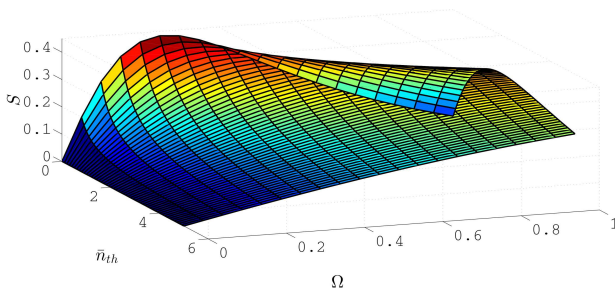


Fig. 8. (Color online). A plot of the quadrature squeezing [Eq. (32)] versus Ω and \bar{n}_{th} for $\gamma_c = 0.4$, and $\gamma = 0.2$

On the other hand, the plots in Fig. 7 show the quadrature squeezing by Eq. (32) versus Ω for $\gamma_c = 0.4$, $\gamma = 0.2$, and for different values of \bar{n}_{th} . From these plots, we see that, for $\bar{n}_{th} = 0.5$, $\bar{n}_{th} = 0.2$, and $\bar{n}_{th} = 0$, the corresponding maximum quadrature squeezings are 36%, 39.3%, and 43.42%. This occurs, when the three-level laser is operating at $\Omega = 0.4343$, $\Omega = 0.3232$, and $\Omega = 0.2626$, respectively.

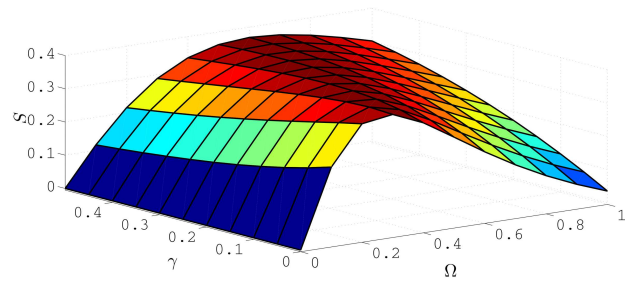


Fig. 9. (Color online). A plot of the quadrature squeezing [Eq. (32)] versus Ω and γ for $\gamma_c = 0.4$ and $\bar{n}_{th} = 0.2$

We observe from Fig. 8 that the squeezing is significantly degraded by the thermal light. Even then, a considerable quadrature squeezing is achievable via controlling the thermal noise entering the cavity by adjusting the transmittance of the mirror. A maximum degree of squeezing of nearly 39.3% occurs, when the cavity is coupled to a thermal reservoir with the mean photon number $\bar{n}_{th} = 0.2$ for $\gamma_c = 0.4$, $\gamma = 0.2$, and $\Omega = 0.3232$. Figure 9 shows the plot of two-mode quadrature squeezing versus Ω and γ for $\gamma_c = 0.4$ and $\bar{n}_{th} = 0.2$. We see from this figure that the degree of two-mode squeezing increases with the the spontaneous emission decay constant γ .

4. Entanglement

In this section, we study the degree of entanglement of photon-states and the atom entanglement of the two-mode cavity light produced by a system under consideration.

4.1. Photon Entanglement

Here, we prefer to analyze the entanglement of photon-states in the laser cavity. Quantum entanglement is a physical phenomenon that occurs, when pairs or groups of particles cannot be described independently. Instead, a quantum state may be given for the system as a whole. Measurements of physical properties such as the position, momentum, spin, polarization, *etc.* performed on entangled particles are found to be appropriately correlated. A pair of particles is taken to be entangled in quantum theory, if its states cannot be expressed as a product of the states of its individual constituents. The preparation and manipulation of these entangled states that have nonclassical and nonlocal properties lead to a bet-

ter understanding of the basic quantum principles. It is in this spirit that this section is devoted to the analysis of the entanglement of the two-mode photon states. In other words, it is a well-known fact that a quantum system is said to be entangled, if it is not separable. In other words, if the density operator for the combined state cannot be described as a combination of the product density operators of the constituents,

$$\hat{\rho} \neq \sum_k p_k \hat{\rho}_k^{(1)} \otimes \hat{\rho}_k^{(2)}, \quad (34)$$

in which $p_k \gg 0$ and $\sum_k p_k = 1$ are related to the normalization of the combined density states. On the other hand, a maximally entangled CV state can be expressed as a co-eigenstate of a pair of EPR-type operators [40] such as $\hat{x}_a - \hat{x}_b$ and $\hat{P}_a - \hat{P}_b$. The total variance of these two operators reduces to zero for maximally entangled CV states. According to the inseparable criteria given by Duan *et al.* [41], cavity photon-states of a system are entangled, if the sum of the variances of a pair of EPR-like operators,

$$\hat{s} = \hat{x}_a - \hat{x}_b, \quad (35)$$

$$\hat{t} = \hat{p}_a + \hat{p}_b, \quad (36)$$

where $\hat{x}_a = (\hat{a} + \hat{a}^\dagger)/\sqrt{2}$, $\hat{x}_b = (\hat{b} + \hat{b}^\dagger)/\sqrt{2}$, $\hat{p}_a = i(\hat{a}^\dagger - \hat{a})/\sqrt{2}$, and $\hat{p}_b = i(\hat{b}^\dagger - \hat{b})/\sqrt{2}$ are quadrature operators for modes a and b , satisfy

$$\Delta s^2 + \Delta t^2 < 2N \quad (37)$$

and recalling the cavity mode operators \hat{a} and \hat{b} are Gaussian variables with zero mean, we readily get

$$\Delta s^2 + \Delta t^2 = 2\Delta c_-^2, \quad (38)$$

where Δc_-^2 is given by (29). One can immediately notice that this particular entanglement measure is directly related to the two-mode squeezing. This direct relationship shows that, whenever there is a two-mode squeezing in the system, there will be entanglement in the system as well. It is noted that the entanglement disappears, when the squeezing vanishes. This is due to the fact that the entanglement is directly related to the squeezing as given by (29). It also follows that, like the mean photon number and quadrature variance, the degree of entanglement depends on the number of atoms. With the help of criterion (37) that a significant entanglement between

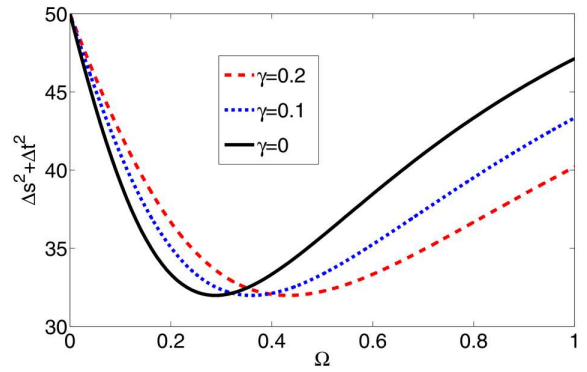


Fig. 10. (Color online). Plots of the photon entanglement of the two-mode cavity light [Eq. (38)] versus Ω for $\gamma_c = 0.4$, $\gamma = 0.2$, and for different values of \bar{n}_{th}

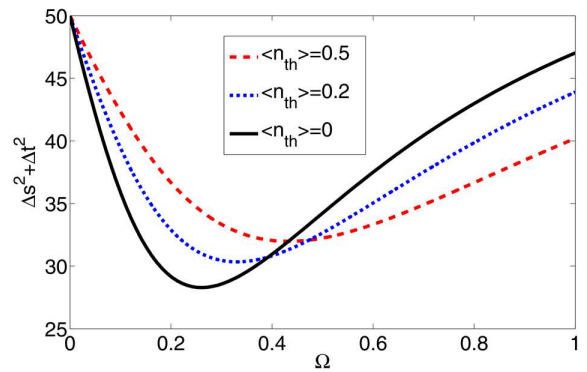


Fig. 11. (Color online). Plots of the photon entanglement of the two-mode cavity light [Eq. (38)] versus Ω for $\gamma_c = 0.4$, $\gamma = 0.2$, and for different values of \bar{n}_{th}

the states of the light generated in the cavity. This is due to the strong correlation between the radiation emitted, when the atoms decay from the upper energy level to the lower one via the intermediate level.

The plots on Fig. 10 show that, as the spontaneous emission decay constant increases, the photon entanglement decreases. Similarly, as we observe from the data of Table 5.1, the photon entanglement is decreased with increasing the spontaneous emission decay constant. From these plots and values of $\kappa = 0.8$, $\gamma_c = 0.4$, $\bar{n}_{\text{th}} = 0.5$, and $N = 50$, we determined the maximum photon entanglement is 36% and it occurs at $\Omega = 0.2929$, $\Omega = 0.3636$, and $\Omega = 0.4343$ for $\gamma = 0$, $\gamma = 0.1$, and $\gamma = 0.2$ respectively.

We observe from the plots in Fig. 11 that, as a thermally seeded light mean photon number value increases, the photon entanglement also increases. Si-

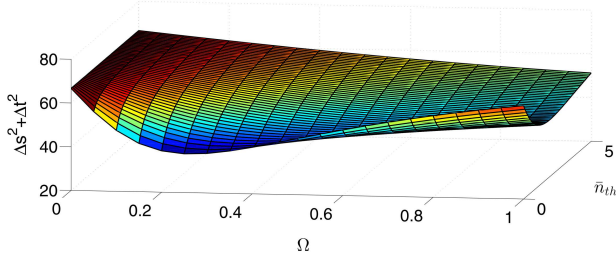


Fig. 12. (Color online). A plot of the photon entanglement of the two-mode cavity light [Eq. (38)] versus Ω and \bar{n}_{th} for $\gamma_c = 0.4$ and $\gamma = 0.2$

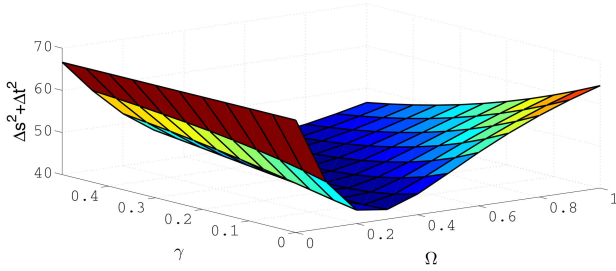


Fig. 13. (Color online). A plot of the photon entanglement of the two-mode cavity light [Eq. (38)] versus Ω and γ for $\gamma_c = 0.4$ and $\bar{n}_{th} = 0.5$

ilarly, as we observe from the data of Table 5.1, the photon entanglement increases with a thermally seeded light mean photon number value. From these plots and the values of $\kappa = 0.8$, $\gamma_c = 0.4$, $\gamma = 0.2$ and $N = 50$, we determined that the maximum photon entanglements are $E = 28.3\%$, $E = 30.34\%$, $E = 32\%$. This occurs at $\Omega = 0.2626$, $\Omega = 0.3232$, and $\Omega = 0.4343$ for $\bar{n}_{th} = 0$, $\bar{n}_{th} = 0.2$, and $\bar{n}_{th} = 0.5$, respectively.

It is clearly shown in Figs. 12 and 13 that the photon entanglement increases, as \bar{n}_{th} and γ decrease, respectively. On both figures, the maximum degree of entanglement occurs for $\Omega = 0.2929$, where the maximum degree of squeezing occurs, as we observe from the plots of Figs. 4 and 5. This indicates that the entanglement is directly related to the two-mode quadrature squeezing.

4.2. Cavity Atomic-States Entanglement

The quantum entanglement between the two cavity modes a and b proposed by Duan, Giedke, Cirac, and Zoller (DGCZ) in [41], which is a sufficient condition for the entangled quantum states. According to DGCZ, a quantum state of the system is said to be entangled, if the sum of the variances of the EPR-like

quadrature operators, \hat{u} and \hat{v} , satisfy the inequality

$$\Delta u^2 + \Delta v^2 < 2N^2. \quad (39)$$

On the other hand, the cavity atomic-states of the system are entangled, if the sum of the variances of a pair of EPR-like operators,

$$\hat{u} = \hat{x}'_a - \hat{x}'_b, \quad (40)$$

$$\hat{v} = \hat{p}'_a + \hat{p}'_b, \quad (41)$$

where $\hat{x}'_a = (\hat{m}_a + \hat{m}_a^\dagger)/\sqrt{2}$, $\hat{x}'_b = (\hat{m}_b + \hat{m}_b^\dagger)/\sqrt{2}$, $\hat{p}'_a = i(\hat{m}_a^\dagger - \hat{m}_a)/\sqrt{2}$, and $\hat{p}'_b = i(\hat{m}_b^\dagger - \hat{m}_b)/\sqrt{2}$ are the atomic quadrature operators. Since \hat{m}_a and \hat{m}_b are Gaussian variables with zero means, one can easily verify that

$$\Delta u^2 + \Delta v^2 = [\langle \hat{m}_a^\dagger \hat{m}_a \rangle + \langle \hat{m}_a \hat{m}_a^\dagger \rangle + \langle \hat{m}_b^\dagger \hat{m}_b \rangle + \langle \hat{m}_b \hat{m}_b^\dagger \rangle - \langle \hat{m}_b^\dagger \hat{m}_a^\dagger \rangle - \langle \hat{m}_a \hat{m}_b \rangle]. \quad (42)$$

It follows that

$$\Delta u^2 + \Delta v^2 = N[N + \langle \hat{N}_a \rangle - 2\langle \hat{m}_c \rangle]. \quad (43)$$

In view of Eqs. (17) and (20), the entanglement of cavity atomic-states of the two-mode cavity light takes, at a steady-state, the form

$$\Delta u^2 + \Delta v^2 = N^2 \left[\frac{(\gamma_c + \gamma)^2 (\bar{n}_{th} + 1) (2\bar{n}_{th} + 1)}{(\gamma_c + \gamma)^2 (\bar{n}_{th} + 1) (2\bar{n}_{th} + 1) + 3\Omega^2} + \frac{4\Omega^2 - 2\Omega(\gamma_c + \gamma)(\bar{n}_{th} + 1)}{(\gamma_c + \gamma)^2 (\bar{n}_{th} + 1) (2\bar{n}_{th} + 1) + 3\Omega^2} \right]. \quad (44)$$

As we see from Eq. (43), the entanglement of cavity atomic-states of the two-mode cavity light strongly depends on the number of atoms.

On the other hand, in the absence of a driving coherent light, $\Omega = 0$, Eq. (44) turns out to be

$$\Delta u^2 + \Delta v^2 = N^2. \quad (45)$$

We see from the plots in Fig. 14 that, as the spontaneous emission decay constant increases, the atom entanglement decreases. This occurs at the same value of Ω . Similarly, as we observe from the data in Fig. 14, the atom entanglement is decreased with increasing the spontaneous emission decay constant γ . From these plots and values of $\kappa = 0.8$, $\gamma_c = 0.4$, $\bar{n}_{th} = 0.5$, and $N = 50$, we determined that the maximum atom entanglement is 36%, and this occurs at

$\Omega = 0.2929$, $\Omega = 0.3636$, and $\Omega = 0.4343$ for $\gamma = 0$, $\gamma = 0.1$, and $\gamma = 0.2$, respectively.

The plots in Fig. 15 indicate that, as a thermally seeded light mean photon number value increases, the atom entanglement also increased. Similarly, as we observe from the plots in this figure, the photon entanglement increases with the thermally seeded light mean photon number. From these plots and the values of $\kappa = 0.8$, $\gamma_c = 0.4$, $\gamma = 0.2$ and $N = 50$, we determined that the maximum atom entanglements are $E = 43.44\%$, $E = 39.32\%$, and $E = 36\%$. This occurs at $\Omega = 0.2626$, $\Omega = 0.3232$, and $\Omega = 0.4343$ for $\bar{n}_{th} = 0$, $\bar{n}_{th} = 0.2$, and $\bar{n}_{th} = 0.5$, respectively.

It is clearly shown in Figs. 16 and 17 that the atom entanglement increases with a decrease in \bar{n}_{th} and γ , respectively. In both figures, the maximum degree of entanglement occurs for $\Omega = 0.2929$ with the maximum degree of squeezing, as we observe from the plots of Figs. 4 and 5. This indicates that, similarly

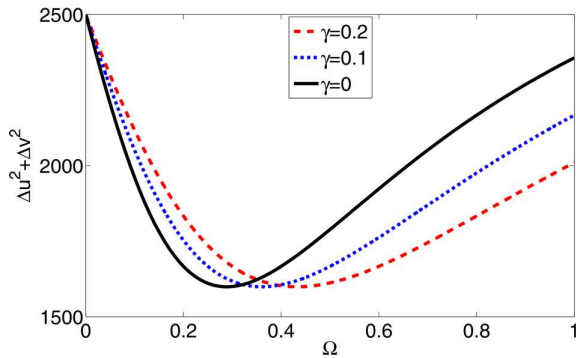


Fig. 14. (Color online). Plots of the atom entanglement of the two-mode cavity light [Eq. (44)] versus Ω for $\gamma_c = 0.4$, $\gamma = 0.2$, and for different values of \bar{n}_{th}

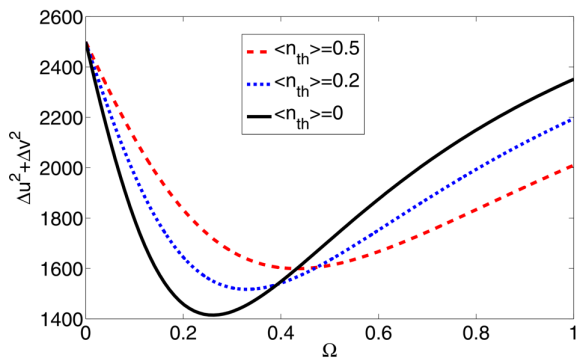


Fig. 15. (Color online). Plots of the atom entanglement of the two-mode cavity light [Eq. (44)] versus Ω for $\gamma_c = 0.4$, $\gamma = 0.2$, and for different values of \bar{n}_{th}

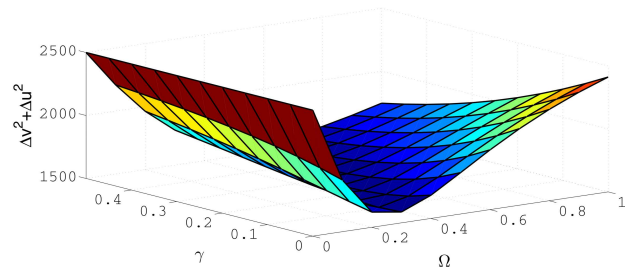


Fig. 16. (Color online). A plot of the atom entanglement of the two-mode cavity light [Eq. (44)] versus γ and Ω for $\gamma_c = 0.4$ and $\bar{n}_{th} = 0.5$

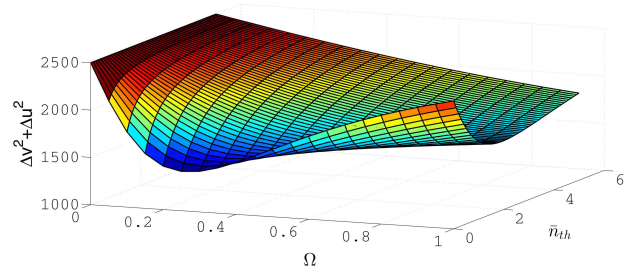


Fig. 17. (Color online). A plot of the atom entanglement of the two-mode cavity light [Eq. (44)] versus Ω and \bar{n}_{th} for $\gamma_c = 0.4$ and $\gamma = 0.2$

to the photon entanglement, the atom entanglement is also directly related to the two-mode quadrature squeezing.

On the basis of criteria (37) and (39), we clearly see that the two states of the generated light are strongly entangled in the steady state. Moreover, the absence of thermal light leads to an increase in the degree of entanglement.

5. Photon Statistics

5.1. The mean photon number

The mean photon number of the two-mode light beam represented by the operators \hat{c} and \hat{c}^\dagger , is defined by

$$\bar{n} = \langle \hat{c}^\dagger \hat{c} \rangle. \quad (46)$$

The steady-state solution of Eq. (16) is

$$\hat{c} = \frac{2g}{\kappa\sqrt{N}}\hat{m}. \quad (47)$$

Hence, in the steady state, the mean photon number goes into

$$\bar{n} = \frac{\gamma_c}{\kappa} \left[\langle \hat{N}_a \rangle + \langle \hat{N}_b \rangle \right]. \quad (48)$$

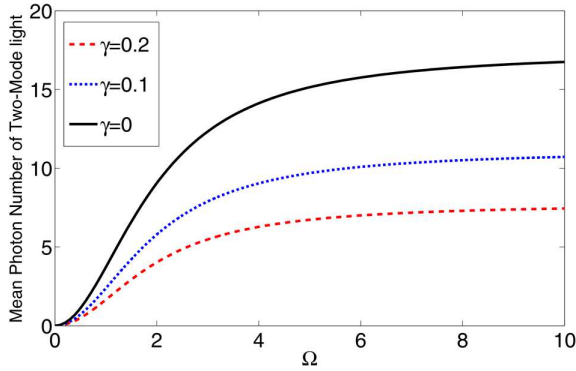


Fig. 18. (Color online). Plots of the mean photon number of the two-mode cavity light [Eq. (49)] versus Ω for $\gamma_c = 0.4$, $\bar{n}_{th} = 0.5$, and for different values of γ

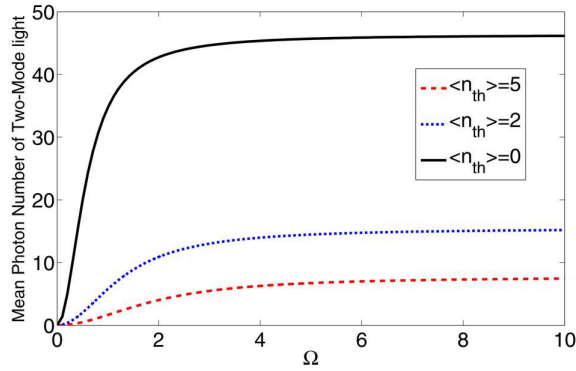


Fig. 19. (Color online). Plots of the mean photon number of the two-mode cavity light [Eq. (49)] versus Ω for $\gamma_c = 0.4$, $\gamma = 0.2$, and for different values of \bar{n}_{th}

It follows that

$$\bar{n} = \frac{\gamma_c}{\kappa} N \left[\frac{2\Omega^2}{(\gamma_c + \gamma)^2(\bar{n}_{th} + 1)(2\bar{n}_{th} + 1) + 3\Omega^2} \right]. \quad (49)$$

The plots in Fig. 18 show that, as the spontaneous emission decay constant γ increases, the global mean photon number of the two-mode cavity light decreases. In addition, the plots in Fig. 18 indicate that, as Ω increases, the mean photon number also increases.

From the plots in Fig. 19, we see that, as the initially seeded thermal light \bar{n}_{th} increases, the global mean photon number of the two-mode cavity light decreases. In addition, the plots in Fig. 19 indicate that, as Ω increases, the mean photon number slightly increases as well. Therefore, the absence of thermal light increases the global mean photon number of the two-mode cavity light beams.

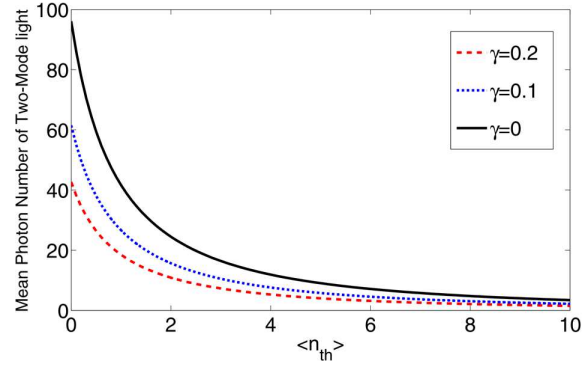


Fig. 20. (Color online). Plots of the mean photon number of the two-mode cavity light [Eq. (49)] versus \bar{n}_{th} for $\gamma_c = 0.4$, $\Omega = 2$, and for different values of γ

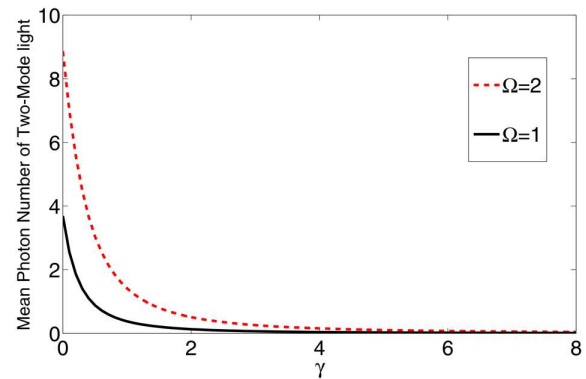


Fig. 21. (Color online). Plots of the mean photon number of the two-mode cavity light [Eq. (49)] versus γ for $\gamma_c = 0.4$, $\bar{n}_{th} = 0.5$, and for different values of Ω

The plots in Fig. 20 describe the global mean photon number of the two-mode light beams versus \bar{n}_{th} for $\gamma_c = 0.4$, $\kappa = 0.8$, $N = 50$, $\Omega = 2$, $\Omega = 2$, and for different values of γ . From these plots, we observe that the global mean photon number of the two-mode cavity light decreases, as γ increases. We can see from the same plots that the mean photon number decreases, as \bar{n}_{th} increases.

We observe from the plots in Fig. 21 that the mean photon number of the two-mode light beam has a higher value for the case $\Omega = 2$ than for $\Omega = 1$. This indicates that the photon number higher in mean depends on the pumping amplitude. This means that a higher pumping gives more bright light. On the other hand, Fig. 21 shows that, as the spontaneous emission decay constant γ increases, the mean photon number decreases.

The plots in Fig. 22 describe the global mean photon number of the two-mode light beams versus \bar{n}_{th} with values of $\gamma_c = 0.4$, $\kappa = 0.8$, $N = 50$, $\Omega = 2$, $\Omega = 2$, and for different values of γ . From these plots we observe that the global mean photon number of the two-mode cavity light decreases as γ increases. We can see also that, from the same plots, the mean photon number decreases, as \bar{n}_{th} increases.

We observe from the plots in Fig. 23 that the mean photon number of the two-mode light beam has greater value for the case $\Omega = 2$ than when $\Omega = 1$. This indicates that the greater in mean photon number is depending on the amplitude of the pumping. This means that the more intense pumping gives brighter light. On the other hand, Fig. 23 shows that, as the spontaneous emission decay constant, γ , increases, the mean photon number decreases.

5.2. The normalized photon number correlation

In order to determine whether the photon numbers of mode a and mode b are correlated or not, we must examine the normalized correlation of photon numbers. Thus, these correlations for light mode a and light mode b can be defined as [3, 28, 37]

$$g_{(a,b)}^{(2)}(t) = \frac{\langle \hat{n}_a \hat{n}_b \rangle}{\langle \hat{n}_a \rangle \langle \hat{n}_b \rangle}, \quad (50)$$

where $\langle \hat{n}_a \rangle = \langle \hat{a}^\dagger \hat{a} \rangle$, $\langle \hat{n}_b \rangle = \langle \hat{b}^\dagger \hat{b} \rangle$, $\langle \hat{n}_a \hat{n}_b \rangle = \langle \hat{a}^\dagger \hat{a} \hat{b}^\dagger \hat{b} \rangle$. Since \hat{a} and \hat{b} are Gaussian variables with zero means, one can verify that

$$g_{(a,b)}^{(2)}(t) = 1 + \frac{\langle \hat{a}^\dagger \hat{b}^\dagger \rangle \langle \hat{a} \hat{b} \rangle + \langle \hat{a}^\dagger \hat{b} \rangle \langle \hat{a} \hat{b}^\dagger \rangle}{\langle \hat{a}^\dagger \hat{a} \rangle \langle \hat{b}^\dagger \hat{b} \rangle}. \quad (51)$$

It then follows that

$$g_{(a,b)}^{(2)}(t) = 1 + \frac{\langle \hat{m}_c \rangle^2}{\langle \hat{N}_a \rangle \langle \hat{N}_b \rangle}. \quad (52)$$

In view of Eqs. (17), (18), and (20), one can show that

$$g_{(a,b)}^{(2)}(t) = 1 + \frac{(\gamma + \gamma_c)^2 (\bar{n}_{\text{th}} + 1)^2}{\Omega^2}. \quad (53)$$

This result indicates that the correlation of photon numbers is different from one. Thus, the photon numbers of mode a and mode b of a pair of two-mode laser light beams are correlated. It can be shown from this

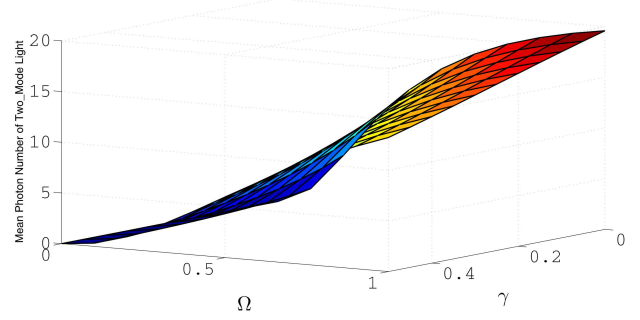


Fig. 22. (Color online). A Plot of the mean photon number of the two-mode cavity light [Eq. (49)] versus γ for $\gamma_c = 0.4$, $\bar{n}_{\text{th}} = 0.5$, and for different values of Ω

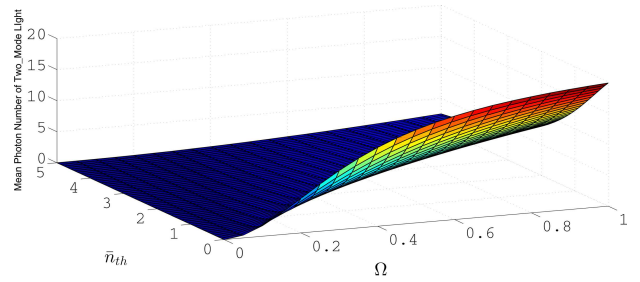


Fig. 23. (Color online). A plot of the mean photon number of the two-mode cavity light [Eq. (49)] versus γ for $\gamma_c = 0.4$, $\bar{n}_{\text{th}} = 0.5$, and for different values of Ω

result that the second-order correlation function of the two-mode light does not depend on the number of atoms. Moreover, we can see from Eq. (52) that the expectation value of the product of number operators, $\langle \hat{n}_a \hat{n}_b \rangle$ is different from $\langle \hat{n}_a \rangle \langle \hat{n}_b \rangle$. This implies that there is an intermode correlation. Thus, this intermode correlation must be due to the atomic coherence induced by the atoms in the coherent coupling of the top and bottom levels.

Moreover, in the absence of a thermal reservoir, ($\bar{n}_{\text{th}} = 0$), the variance of the intensity difference for this case has the form

$$g_{(a,b)}^{(2)}(t) = 1 + \frac{\gamma_c^2}{\Omega^2}. \quad (54)$$

Now, it is essential to calculate the second-order correlation function for the individual mode to have an insight for the previous result. To this end, the second-order correlation function for mode a is given by

$$g_{(a,a)}^{(2)}(0) = \frac{\langle : \hat{n}_a \hat{n}_a : \rangle}{\langle \hat{n}_a \rangle^2}, \quad (55)$$

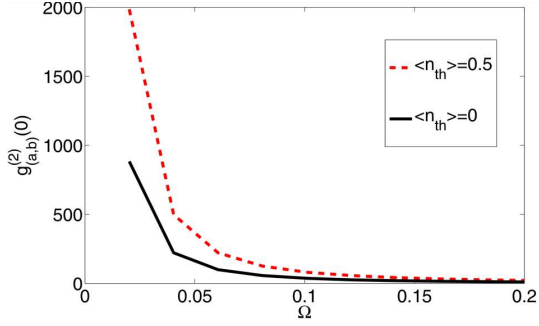


Fig. 24. (Color online). Plots of $g_{(a,b)}^{(2)}(0)$ of the two-mode cavity light versus Ω for $\gamma_c = 0.4$, $\gamma = 0.2$, and for different values of \bar{n}_{th}

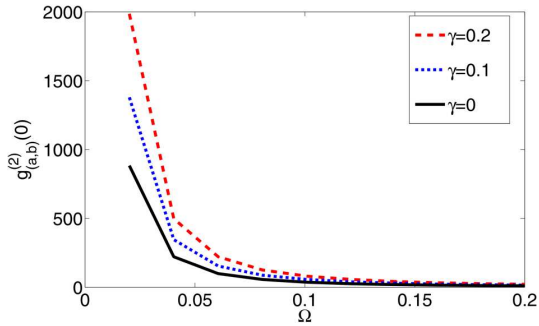


Fig. 25. (Color online). Plots of $g_{(a,b)}^{(2)}(0)$ of the two-mode cavity light versus Ω for $\gamma_c = 0.4$, $\gamma = 0.2$, and for different values of \bar{n}_{th}

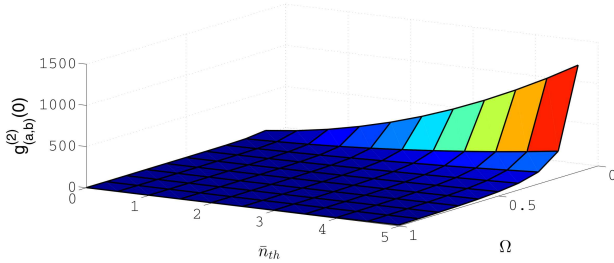


Fig. 26. (Color online). A plot of $g_{(a,b)}^{(2)}(0)$ of the two-mode cavity light versus Ω for $\gamma_c = 0.4$, $\gamma = 0.2$, and for different values of \bar{n}_{th}

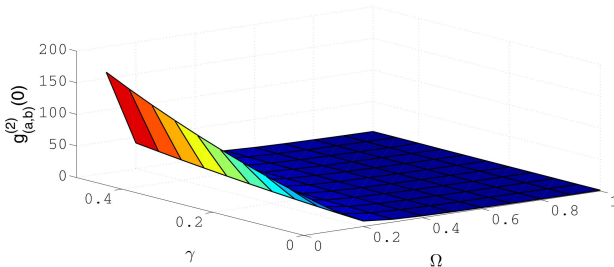


Fig. 27. (Color online). A plot of $g_{(a,b)}^{(2)}(0)$ of the two-mode cavity light versus Ω for $\gamma_c = 0.4$, $\gamma = 0.2$, and for different values of \bar{n}_{th}

where $::$ represent the normal ordering, and $\hat{n}_a = \hat{a}^\dagger \hat{a}$ is the photon number operator for mode a . Since \hat{a} is a Gaussian variable with vanishing mean, one can easily verify that

$$g_{(a,a)}^{(2)}(0) = 2. \quad (56)$$

Similarly, the second-order correlation function for mode b is found to be

$$g_{(b,b)}^{(2)}(0) = 2. \quad (57)$$

From expressions (56) and (57), we note that the second-order correlation function for light indicates a chaotic state. So, the cavity modes a and b are separately in a chaotic or thermal state.

Figure 24 shows that the second-order correlation function for the two-mode light versus Ω in the presence ($\gamma \neq 0$) and absence ($\gamma = 0$) of the spontaneous emission. One can see from this figure that $g_{(a,b)}^{(2)}(0)$ decreases, when Ω increases, in both cases. It can be observed from Figs. 24 and 25 that the second-order correlation function vanishes for $\Omega < 0.05$. Moreover, the effect of the spontaneous emission is an increase in the second-order correlation function. In addition, it is clearly shown in Figs. 26 and 27 that the second-order correlation function increases with \bar{n}_{th} and γ , respectively. In both figures, the maximum degree of second-order correlation function occurs at the minimum value of Ω .

Furthermore, in order to quantify the correlation between the two modes, we introduce the linear correlation coefficient in terms of a covariance as [11]

$$J_{(\hat{n}_a, \hat{n}_b)} = \frac{\text{cov}(\hat{n}_a, \hat{n}_b)}{\sqrt{\Delta \hat{n}_a^2} \sqrt{\Delta \hat{n}_b^2}}, \quad (58)$$

where $\Delta \hat{n}_a^2$ and $\Delta \hat{n}_b^2$ are the variances of the photon number for modes a and b , respectively. So, the covariance of the photon numbers is defined by

$$\text{cov}(\hat{n}_a, \hat{n}_b) = \langle \hat{n}_a \hat{n}_b \rangle - \langle \hat{n}_a \rangle \langle \hat{n}_b \rangle. \quad (59)$$

One can easily verify, using the fact that \hat{a} and \hat{b} are Gaussian variables, in the steady state that

$$\text{cov}(\hat{n}_a, \hat{n}_b) = \langle \hat{b} \hat{a} \rangle_{ss} \langle \hat{a}^\dagger \hat{b}^\dagger \rangle_{ss}. \quad (60)$$

Since the cavity modes are separately in a chaotic state the variances of the photon numbers obey the relation for a chaotic state,

$$\Delta \hat{n}_a^2 = \langle \hat{n}_a \rangle + \langle \hat{n}_a \rangle^2, \quad (61)$$

$$\Delta \hat{n}_b^2 = \langle \hat{n}_b \rangle + \langle \hat{n}_b \rangle^2. \quad (62)$$

In view of this fact and (60), the correlation function can be rewritten as

$$J_{(\hat{n}_a, \hat{n}_b)} = \frac{\langle \hat{b} \hat{a} \rangle_{ss} \langle \hat{a}^\dagger \hat{b}^\dagger \rangle_{ss}}{\sqrt{\langle \hat{n}_a \rangle_{ss} + \langle \hat{n}_a \rangle_{ss}^2} \sqrt{\langle \hat{n}_b \rangle_{ss} + \langle \hat{n}_b \rangle_{ss}^2}}. \quad (63)$$

In Figure 28, the linear correlation coefficient versus the amplitude of the driving coherent light, Ω is plotted. It is also found from this figure that for Ω very close to 0 the intermode correlation would be significantly large, since the mean photon numbers of the light in modes b is very close to zero, when almost all atoms are initially populated in the lower level. Moreover, similarly to the second-order correlation function, the plots of Figure 28 show that the linear correlation coefficient vanishes, when $\Omega < 0.05$.

5.3. Intensity difference Fluctuations

On the other hand, the variance of the intensity difference can be defined as

$$\Delta I_D^2 = \langle \hat{I}_D^2 \rangle - \langle \hat{I}_D \rangle^2, \quad (64)$$

where the intensity difference is

$$\hat{I}_D = \hat{a}^\dagger \hat{a} - \hat{b}^\dagger \hat{b}. \quad (65)$$

Hence, making use of Eq. (65), the variance of the intensity difference can finally take the form

$$\Delta I_D^2 = \langle \hat{a}^\dagger \hat{a} \rangle [1 + \langle \hat{a}^\dagger \hat{a} \rangle] + \langle \hat{b}^\dagger \hat{b} \rangle [1 + \langle \hat{b}^\dagger \hat{b} \rangle] - 2 \langle \hat{a} \hat{b} \rangle. \quad (66)$$

It then follows that

$$\Delta I_D^2 = \frac{2\gamma_c}{\kappa} [\langle \hat{N}_a \rangle + \langle \hat{N}_a \rangle^2 - \langle \hat{n}_c \rangle^2]. \quad (67)$$

On account of Eqs. (17) and (20), Eq. (67) can be rewritten as

$$\begin{aligned} \Delta I_D^2 &= \\ &= \frac{2\gamma_c}{\kappa} \left[\frac{N\Omega^2((\gamma_c + \gamma)^2(\bar{n}_{th} + 1)(2\bar{n}_{th} + 1) + 3\Omega^2)}{((\gamma_c + \gamma)^2(\bar{n}_{th} + 1)(2\bar{n}_{th} + 1) + 3\Omega^2)^2} \right] + \\ &+ \frac{2\gamma_c}{\kappa} \left[\frac{N^2\Omega^4 - 2\Omega^2 N^2(\gamma_c + \gamma)^2(\bar{n}_{th} + 1)^2}{((\gamma_c + \gamma)^2(\bar{n}_{th} + 1)(2\bar{n}_{th} + 1) + 3\Omega^2)^2} \right]. \quad (68) \end{aligned}$$

This is the steady-state variance of the intensity difference produced by the coherently driven nondegenerate three-level laser with an open cavity and coupled to a two-mode thermal reservoir.

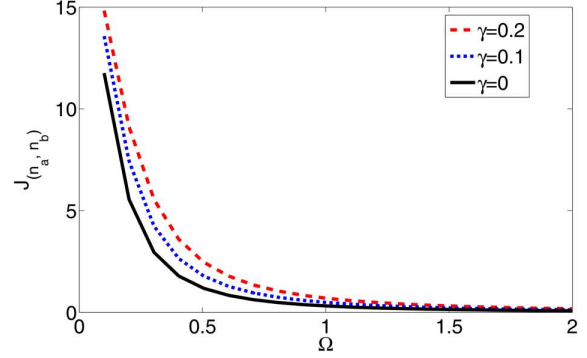


Fig. 28. (Color online). Plots of $J_{(\hat{n}_a, \hat{n}_b)}$ of the two-mode cavity light at steady-state versus Ω for $\gamma_c = 0.4$, $\kappa = 0.8$, $N = 50$, and for different values of γ

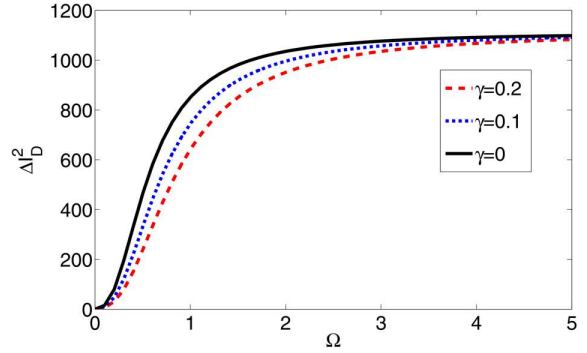


Fig. 29. (Color online). Plots of ΔI_D^2 of the two-mode cavity light at steady-state versus Ω for $\gamma_c = 0.4$, $\kappa = 0.8$, $N = 50$, $\bar{n}_{th} = 5$, and for different values of γ

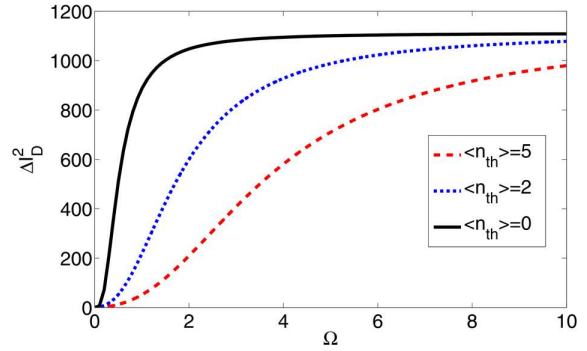


Fig. 30. (Color online). Plots of ΔI_D^2 of the two-mode cavity light at steady-state versus Ω for $\gamma_c = 0.4$, $\kappa = 0.8$, $N = 50$, $\gamma = 0.2$, and for different values of \bar{n}_{th}

The plots of Fig. 29 show the variance of the intensity difference (ΔI_D^2) versus Ω for $\gamma_c = 0.4$, $\kappa = 0.8$, $N = 50$, $\bar{n}_{th} = 5$, and for different values of γ . From these results, we understand that the variance of

the intensity difference increases with Ω . In addition, the variance of the intensity difference also increases, when the spontaneous emission decay constant (γ) decreases.

On the other hand, from Fig. 30, we see the plots of the variance of the intensity difference (ΔI_D^2) of the two-mode cavity light in the steady state versus Ω for $\gamma_c = 0.4$, $\kappa = 0.8$, $N = 50$, $\gamma = 0.2$, and for different values of \bar{n}_{th} . These plots indicate that the variance of the intensity difference decreases, as the initially seeded thermal light increases. In addition, the variance of the intensity difference increases with Ω .

6. Conclusions

In conclusion, the squeezing and entanglement properties of a non-degenerate three-level laser driven by coherent light and coupled to a two-mode thermal reservoir via a single-port mirror whose open cavity contains N nondegenerate three-level atoms, are thoroughly analyzed. It is carried out the analysis by putting the noise operators associated with the thermal reservoir in the normal order and by considering the interaction of the three-level atoms with the thermal reservoir outside the cavity. The master equation and the quantum Langevin equations for the cavity light is obtained. Applying these equations, the equations of evolution of the cavity mode and the atomic operators are solved. Making use of the steady-state solutions of atomic and cavity mode operators, the quadrature variance, the quadrature squeezing, and the entanglement for the two-mode cavity light, at steady state, are determined. In addition, the normalized second-order correlation function is obtained for the individual mode, as well as for the superposition of the two modes. Moreover, it is obtained that the linear correlation coefficient between the two modes. Finally, we obtained the intensity difference fluctuations.

The analysis showed that the intracavity quadrature squeezing is enhanced due to the absence of a spontaneous emission, as well as the initially seeded thermal light. It is found that the squeezing and entanglement in the two-mode light are directly related to each other. As a result, an increase in the degree of squeezing directly implies an increase in the degree of entanglement and vice versa. This shows that whenever there is squeezing in the two-mode light, there exists the entanglement in the system. In addition, it is shown that the photons in the laser cavity

are highly correlated, and the degree of photon number correlation increases with the spontaneous emission decay constant, γ . Therefore, the presence of the spontaneous emission leads to an increase in the degrees of entanglement, squeezing and photon number correlation.

It is found that the maximum quadrature squeezing is 43.43% in the absence of thermal light. When the thermal light intensity increases, the squeezing decreases. Moreover, we found that the mean photon number increases, as the spontaneous emission decreases. Therefore, the more the mean photon number, the higher the light brightness. Hence, the absence of a spontaneous emission gives bright and squeezed light beams. On the other hand, the thermal reservoir causes a decrease in both the mean photon number and the squeezing.

1. M.O. Scully, M.S. Zubairy. *Quantum Optics* (Cambridge University Press, 1997).
2. F. Kassahun. *Refind Quantum Analysis of Light* (Create Space Independent Publishing Platform, 2014).
3. K. Fesseha. Three-level laser dynamics with squeezed light. *Phys. Rev. A* **63**, 033811 (2001).
4. M.O. Scully, M.S. Zubairy. Noise free amplification via the two-photon correlated spontaneous emission laser. *Opt. Commun.* **66**, 303 (1988).
5. J. Anwar, M.S. Zubairy. Quantum-statistical properties of noise in a phase-sensitive linear amplifier. *Phys. Rev. A* **49**, 481 (1994).
6. N. Lu, F.X. Zhao, J. Bergou. Nonlinear theory of a two-photon correlated-spontaneous-emission laser: A coherently pumped two-level-two-photon laser. *Phys. Rev. A* **39**, 5189 (1989).
7. Eyob Alebachew and K. Fesseha. Interaction of a two-level atom with squeezed light. *Opt. Commun.* **271**, 154 (2007).
8. Fesseha Kassahun. Stimulated emission by two-level atoms pumped to the upper level. *Opt. Commun.* **284**, 1357 (2011).
9. N.A. Ansari, J. Gea-Banaclache, M.S. Zubairy. Phase-sensitive amplification in a three-level atomic system. *Phys. Rev. A* **41**, 5179 (1990).
10. N.A. Ansari. Effect of atomic coherence on the second and higher-order squeezing in a two-photon three-level cascade atomic system. *Phys. Rev. A* **48**, 4686 (1993).
11. T. Abebe. The quantum analysis of a non-degenerate three-level laser with spontaneous emission and noiseless vacuum reservoir. *Ukr. J. Phys.* **63** (11), 969 (2018).
12. S.M. Barnett, P.M. Radmore. *Methods in Theoretical Quantum Optics* (Oxford University Press, 1997) [ISBN: 9780198563617].
13. M.O. Scully, K. Wodkiewicz, M.S. Zubairy, J. Bergou, N. Lu, J. Meyer ter Vehn. Two-photon correlated-spon-

- aneous-emission laser: Quantum noise quenching and squeezing. *Phys. Rev. Lett.* **60**, 1832 (1988).
14. T. Abebe. Enhancement of squeezing and entanglement in a non-degenerate three-level cascade laser with coherently driven cavity. *Ukr. J. Phys.* **63** (8), 733 (2018).
 15. C.W. Gardiner, P. Zoller. *Quantum Noise* (Springer Series in Synergetics, 2000)
 16. D.F. Walls. Squeezed states of light. *Nature* **306**, 141 (1983).
 17. C.M. Caves. On the measurement of a weak classical force coupled to a quantum-mechanical oscillator. *Rev. Mod. Phys.* **52**, 341 (1980).
 18. A. Abramovici *et al.* The laser interferometer gravitational-wave observatory. *Science* **256**, 325 (1992).
 19. J. Harms *et al.* Squeezed-input, optical-spring, signal-recycled gravitational-wave detectors. *Phys. Rev. D* **68**, 042001 (2003).
 20. R. Schnabel *et al.* Squeezed light and laser interferometric gravitational Wave detectors. *Classical Quant. Grav.* **25**, 1045 (2004).
 21. C.M. Caves. Quantum-mechanical noise in an interferometer. *Phys. Rev. D* **23**, 1693 (1981).
 22. M. Xiao *et al.* Precision measurement beyond the shot-noise limit. *Phys. Rev. Lett.* **59**, 278 (1987).
 23. E.S. Polzik *et al.* Spectroscopy with squeezed light. *Phys. Rev. Lett.* **68**, 3020 (1992).
 24. Y. Yamamoto, H.A. Haus. Preparation, measurement and information capacity of optical quantum states. *Rev. Mod. Phys.* **58**, 1001 (1986).
 25. R.E. Slusher, L.W. Hollberg, B. Yurke, J.C. Mertz, J.F. Valley. Observation of squeezed states generated by four-wave mixing in an optical cavity. *Phys. Rev. Lett.* **56**, 788 (1986).
 26. K. Fesseha. Three-level laser dynamics with squeezed light. *Phys. Rev. A* **63**, 033811 (2001).
 27. T. Abebe. Coherently driven nondegenerate three-level laser with noiseless vacuum reservoir. *Bulg. J. Phys.* **45**, 357 (2018).
 28. F. Kassahun. *Fundamentals of Quantum Optics* (Lulu, 2008).
 29. N. Lu, S.Y. Zhu. Quantum theory of a two-mode two-photon correlated spontaneous-emission laser. *Phys. Rev. A* **41**, 2865 (1990).
 30. C.A. Blockely, D.F. Walls. Intensity fluctuations in a frequency down-conversion process with three-level atoms. *Phys. Rev. A* **43**, 5049 (1991).
 31. E. Alebachew. Continuous-variable entanglement in a non-degenerate three-level laser with a parametric oscillator. *Phys. Rev. A* **76**, 023808 (2007).
 32. N.A. Ansari. Theory of a two-mode phase-sensitive amplifier. *Phys. Rev. A* **46**, 1560 (1992).
 33. G.S. Agrawal, G. Adam. Photon distributions for nonclassical fields with coherent components. *Phys. Rev. A* **39**, 6259 (1989).
 34. S.M. Barnett, P.M. Radmore. *Methods in Theoretical Quantum Optics* (Oxford University Press, 1997).
 35. N. Lu, S.Y. Zhu. Quantum theory of two-photon correlated-spontaneous-emission lasers: Exact atom-field interaction Hamiltonian approach. *Phys. Rev. A* **40**, 5735 (1989).
 36. E. Alebachew. Enhanced squeezing and entanglement in a non-degenerate three-level cascade laser with injected squeezed light. *Opt. Commun.* **280**, 133 (2007).
 37. S. Tesfa. Dynamics of the cavity radiation of a correlated emission laser initially seeded with a thermal light. *Phys. Scr.* **84**, 045403 (2011).
 38. S. Tesfa. Entanglement amplification in a nondegenerate three-level cascade laser. *Phys. Rev. A* **74**, 043816 (2006).
 39. B.C. Sanders. Entangled coherent states. *Phys. Rev. A* **45**, 6811 (1992).
 40. A. Einstein, B. Podolsky, R. Rosen. Can quantum mechanical description of physical reality be considered complete? *Phys. Rev.* **47**, 777 (1935).
 41. L.M. Duan, G. Giedke, J.J. Cirac, P. Zoller. Inseparability criterion for continuous variable systems. *Phys. Rev. Lett.* **A 84**, 2722 (2000).

Received 17.02.20

Б. Алему, К. Гауу, Е. Мосіса, Т. Абебе

ДИНАМІКА КОРЕЛЬОВАНОГО
ВИПРОМІНЮВАННЯ РЕЗОНАТОРА
ЛАЗЕРА, ПОЄДНАНОГО З ДВОМОДОВИМ
ТЕПЛОВИМ РЕЗЕРВУАРОМ

Аналізуються квантові властивості променя світла із резонатора когерентно збуджуваного невиродженого трирівневого лазера, поєднаного з двомодовим тепловим резервуаром. Аналіз виконано із застосуванням нормально впорядкованих операторів шуму теплового резервуара. Обговорюється вплив теплового та спонтанного випромінювань на динаміку квантових процесів. Показано, що максимальна ступінь стиснення у порожнині на 43% нижче рівня для вакуумного стану. Більше того, наявність теплового випромінювання викликає зменшення ступеня переплутування.

Ключові слова: стимульоване випромінювання, статистика фотонів, квадратурне стиснення, спонтанне випромінювання.